Materials and Design 168 (2019) 107606

Contents lists available at ScienceDirect

Materials and Design

journal homepage: www.elsevier.com/locate/matdes

Design of biomimetic collagen matrices by reagent-free electron beam induced crosslinking: Structure-property relationships and cellular response

Stefanie Riedel [a,b,*,1], Philine Hietschold [a,c,1], Catharina Krömmelbein [a,b], Tom Kunschmann [d], Robert Konieczny [a], Wolfgang Knolle [a], Claudia T. Mierke [d], Mareike Zink [c], Stefan G. Mayr [a,b]

[a] Leibniz Institute of Surface Engineering (IOM), Permoserstr. 15, 04318 Leipzig, Germany
[b] Division of Surface Physics, Department of Physics and Earth Sciences, University of Leipzig, Linnéstr. 5, 04103 Leipzig, Germany
[c] Soft Matter Physics Division, Department of Physics and Earth Sciences, University of Leipzig, Linnéstr. 5, 04103 Leipzig, Germany
[d] Biological Physics Division, Department of Physics and Earth Sciences, University of Leipzig, Linnéstr. 5, 04103 Leipzig, Germany

HIGHLIGHTS

- Collagen hydrogels can be effectively tuned by reagent-free electron treatment to develop biomimetic ECM systems.
- Properties of collagen hydrogels can be tuned by electron treatment influencing pore size and elastic behavior.
- Electron beam treatment excellently maintains chemical integrity of collagen hydrogels.
- Fibroblasts show high cytocompatibility with electron beam treated collagen hydrogels.

GRAPHICAL ABSTRACT

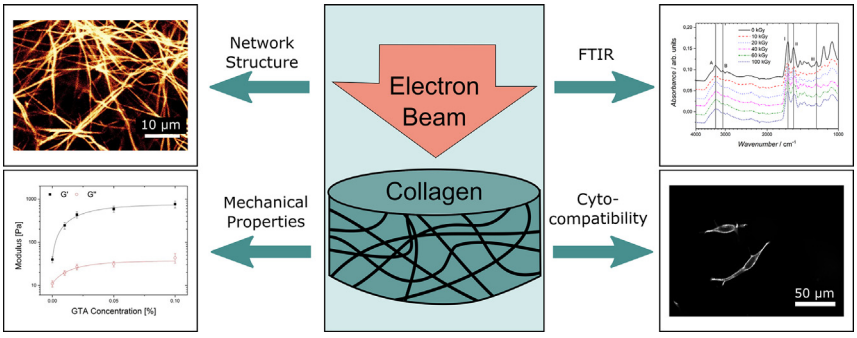

ARTICLE INFO

Article history:
Received 21 September 2018
Received in revised form 11 January 2019
Accepted 14 January 2019
Available online 7 February 2019

Keywords:
Biomimetic collagen
Extracellular matrix model
Reagent-free crosslinking
High energy electron crosslinking

ABSTRACT

Novel strategies to mimic mammalian extracellular matrix (ECM) in vitro are desirable to study cell behavior, diseases and new agents in drug delivery. Even though collagen represents the major constituent of mammalian ECM, artificial collagen hydrogels with characteristic tissue properties such as network size and stiffness are difficult to design without application of chemicals which might be even cytotoxic. In our study we investigate how high energy electron induced crosslinking can be utilized to precisely tune collagen properties for ECM model systems. Constituting a minimally invasive approach, collagen residues remain intact in the course of high energy electron treatment. Quantification of the 3D pore size of the collagen network as a function of irradiation dose shows an increase in density leading to decreased pore size. Rheological measurements indicate elevated storage and loss moduli correlating with an increase in crosslinking density. In addition, cell tests show well maintained viability of NIH 3T3 cells for irradiated collagen gels indicating excellent cellular acceptance. With this, our investigations demonstrate that electron beam crosslinked collagen matrices have a high potential as precisely tunable ECM-mimetic systems with excellent cytocompatibility.

* Corresponding author at: Leibniz Institute of Surface Engineering (IOM), Permoserstr. 15, 04318 Leipzig, Germany.
E-mail addresses: stefanie.riedel@iom-leipzig.de (S. Riedel), stefan.mayr@iom-leipzig.de (S.G. Mayr).
[1] Authors contributed equally.

https://doi.org/10.1016/j.matdes.2019.107606

1. Introduction

In vitro models mimicking mammalian extracellular matrix (ECM) are highly relevant to study cellular behavior [1], tissue development [2] as well as numerous diseases [3], including cancer progression [4,5]. They also can be employed as novel platforms for exploring new drugs [6,7] and agents by reducing extensive and ethically questionable animal experiments. However, besides the specific chemical composition of ECM models, also mechanical properties and network organization (e.g. network pore size) play a crucial role due to their impact on cell proliferation and motility [8–10]. Thus, precise tools for tailoring these model systems are highly desirable to mimic biological ECM.

Among ECM model systems, synthetic polymers are interesting candidates due to their simplicity and reproducibility [11,12]. However, they frequently do not represent physiological environments due to a lack in biophysical and biochemical complexity [13,14]. Natural materials which are derived from in vivo systems are more physiological and thereby might reveal an excellent biocompatibility and biodegradability. Two materials of this category are Matrigel® composed of basement membrane proteins and collagen [15–18]. Collagen is the major component of the mammalian ECM with collagen type I representing the most relevant collagen type occurring in a variety of connective tissue such as tendon, ligaments as well as epithelial tumors [19]. Nowadays, collagen is mainly applied in tissue replacement [20,21], regenerative medicine [22,23], cell culture [24,25] as well as wound dressing applications [26,27]. To this end, collagen is an ideal starting point for artificial ECM models, that also pose the possibility for further fine-tuning based on addition of specific proteins, including elastin, fibronectin and proteoglycans [28]. To tune collagen gels towards physiological ECM models with specific mechanical cues, network architecture, thermal stability and swelling behavior, precise and non-cytotoxic crosslinking methods are required [29]. As common techniques utilize agents such as aldehydes [30,31], epoxides [32] or enzymatic crosslinkers [33] that might adversely affect cell behavior, reagent-free techniques are highly advantageous. Among them, electron irradiation is highly effective to crosslink polymeric hydrogels [34]. Thereby, macro- and •OH-radicals are formed by homolytic scission of bonds at the polymer chain and radiolysis of water molecules, respectively [35]. The •OH-radicals further attack the polymer chains resulting in additional macro-radicals. The macro-radicals are highly reactive and recombine by formation of covalent bonds forming crosslinks in the polymeric network.

Compared to crosslinking techniques utilizing chemical crosslinking agents, electron irradiation promises high efficiency as well as precise and fast crosslinking while not inducing cytotoxicity [36]. It furthermore sterilizes the material on the fly which ensures biomedical application [37]. Within the group of ionizing irradiation, electron irradiation is highly advantageous for modification of hydrogels due to large penetration depths [38] and high dose rates [39] enabling homogeneous crosslinking. In addition, it allows precise global as well as local crosslinking by using a highly focused electron beam, which opens up a multitude of applications ranging from mechanical patterning to actuators [40–42].

In the following, we show that electron irradiation is an effective and precise tool to modify collagen properties. Thereby, we do not focus on thermal properties since they were already intensively studied [43]. Instead, we extend these investigations by characterizing electron beam crosslinked collagen gels in terms of network structure (pore size), rheological properties and cytocompatibility for future biomedical applications such as ECM model systems.

2. Experimental

2.1. Collagen preparation

Collagen gels were synthesized as reported by Kunschmann et al. [44] and Fischer et al. [45] In doing so, collagen gels with a final collagen concentration of 1, 2 and 3 mg/ml were prepared from rat tail collagen (Collagen R, 0.4% solution, Cat. No. 47256.01; SERVA Electrophoresis, Germany) and bovine skin collagen (Collagen G, 0.4% solution, Cat. No. L 7213; Biochrom, Germany) in a ratio of 1:2, respectively. This specific mixing ratio was used because the formed network strongly resembles human collagen networks [45,46]. The collagen solution was prepared on ice to avoid polymerization and was gently mixed until homogeneity. A phosphate buffer containing Na_2HPO_4 (Cat. No. 71636; Sigma-Aldrich Chemie GmbH, Germany) and NaH_2PO_4 (Cat. No. 71507; Sigma-Aldrich Chemie GmbH) was added to obtain a pH of 7.5 and a total phosphate molarity of 200 mM in all gels. The collagen samples polymerized at 37 °C and 100% humidity for 24 h. The samples were rinsed twice and stored in distilled water at room temperature (RT) until use.

2.2. Electron beam treatment

Collagen samples were irradiated using a 10 MeV linear electron accelerator (MB10-30MP; Mevex Corp., Canada). The electron accelerator is equipped with a moving stage with a maximum speed of 3 m/min and a scanning horn with scanning frequency of 3 Hz. The pulse repetition rate was 180 Hz and the pulse length was 8 μs. Final doses were obtained in steps of 5 kGy in accordance to Wisotzki et al. [47] The doses were measured with respect to a graphite dosimeter to an uncertainty of 5%. During electron beam treatment, the samples were cooled to RT by draft to prevent overheating and thereby induced degradation. After irradiation, the samples were stored at 37 °C and 100% humidity for 48 h and later at RT.

2.3. FTIR spectroscopy

Irradiated collagen samples were air dried at ambient conditions for three days. The absorption spectra were measured with a Bruker FTIR (1FS 55 Equinox; Billerica, MA, USA) combined with a mercury cadmium telluride detector and Golden Gate single-reflection diamond attenuated total reflection accessory. 32 scans were performed per measurement.

2.4. Network imaging

To determine the structure of the collagen networks, confocal laser scanning microscopy (CLSM) was utilized and 3D images of the network were analyzed. Collagen gels were first applied onto coverslips which were coated to improve collagen adhesion. In doing so, glass surfaces were hydroxylated by annealing at 120 °C for 2 h. After cooling down, they were silanized with (3-Aminopropyl)trimethoxysilane (97%, Cat. No. 281778; Sigma-Aldrich Chemie GmbH). After drying for 5 min, glasses were washed three times with distilled water. Subsequently, glutaraldehyde (2.5%, Cat. No. G6257; Sigma-Aldrich Chemie GmbH) was added for 20 min to functionalize the surface. Finally, the collagen solution was applied onto the cover-glasses. After polymerization, collagen samples were washed three times with distilled water and irradiated as described before. Gels were then fluorescently stained over night with 5/6-carboxytetramethylrhodamine succinimidyl ester (50 μg\ml, 5/6-TAMRA(SE), Cat. No. 90022; BIOTREND Chemikalien GmbH, Germany). Afterwards, staining solution was removed and samples were washed three times and then stored in distilled water. During the whole staining process, exposure to light was avoided to prevent bleaching.

To image the network structure, a CLSM (TCS SP2; Leica Microsystems, Germany) was utilized. A helium-neon laser (wavelength 543 nm) was employed to excite the fluorescent 5/6-TAMRA(SE) (ex./em. wavelength: 540/565 nm). Collagen was then imaged in 3D. For each collagen concentration three coverslips were prepared and three positions per coverslip were imaged and analyzed.

2.5. Network pore size

To determine the pore size of the collagen networks, the CLSM image stacks were analyzed (Fig. 1(a)). After binarization of the CLSM images

(Fig. 1(b)), the 3D euclidean distances to the nearest fiber were determined for every voxel, similar to Mickel et al. [48] A corresponding distance map shows local maxima representing the center of a pore (Fig. 1(c)). Thereby, the euclidean distance of the local maximum correlates to the radius of that pore. The diameter is then characterized as the pore size. A distribution of all occurring pore sizes is then used to evaluate the characteristic pore size which is defined as the mean of the distribution (Fig. 1(d)). Significance of pore sizes was tested by an independent two-sample *t*-test.

2.6. Rheology

The viscoelastic properties were determined by a MCR-300 bulk rheometer (Anton Paar; Austria) with a 10 mm-diameter parallel-plate geometry. Samples with diameters of 10 mm were cut out of collagen sheets with a height of approx. 3 mm. All measurements were performed in a temperature controlled environment at 25 °C. The strain independent region in the range of 0.01% to 5% was determined by strain sweeps at 1 Hz (not shown here). The storage and loss moduli were then measured by frequency sweeps. The characteristic elastic modulus was then determined at 1 Hz and at 1% strain (in the strain independent region as determined before). In total, ten samples per treatment method were measured while one measurement per sample was performed to exclude dehydration effects.

The degree of crosslinking ν_c was roughly estimated by rubber elasticity theory using the following relationship between storage modulus G′, gas-constant R and temperature T: [49]

$$G' = \nu_c RT. \quad (1)$$

2.7. Cellular response

To assess cytocompatibility, NIH 3T3 mouse fibroblasts (CRL-1658; ATCC, Germany) were cultured on irradiated collagen as well as on unirradiated gels as control. After washing the gels directly after irradiation with phosphate buffered saline (PBS), they were incubated with cell culture medium (90% DMEM, FG0435; Biochrom & 10% calf serum, 26010075; Thermofischer, Germany) and Pen/Strep (1% 10.000 U/ml, A2212; Biochrom) for 4 days. Before seeding cells onto the gels, medium was removed and fresh medium was applied.

Cells were pre-cultured in standard cell culture dishes and detached by Trypsin/EDTA (0.025%/0.01%, L2143; Biochrom). Trypsin was inhibited by serum-containing cell-medium. After centrifugation (90 RCF, 4 min) and removal of supernatant, the collected cells were resuspended in medium and the cell density was determined via cell-counting-chamber. In each well (surface area of 9.5 cm^2), approx. 70.000 and 50.000 cells were cultured for 48 and 72 h at 37 °C, 5% CO_2 and 100% humidity for cell imaging and viability measurements, respectively.

Cell imaging was performed by fluorescent actin staining. In doing so, the cells were fixed using paraformaldehyde (PFA; HT5011; Sigma-Aldrich Chemie GmbH) at RT. After washing twice with PBS, cells were incubated with Triton X-100 in PBS (0.1%, X100; Sigma-Aldrich Chemie GmbH) for 20 min at 8 °C. After washing twice with PBS, the gels were incubated at RT with serum albumin in PBS (BSA, 1%, A2153; Sigma-Aldrich Chemie GmbH). Afterwards, actin was stained by Alexa Fluor™ 488 Phalloidin (A12379; Thermofischer). Phalloidin (300 units) was diluted in methanol (1.5 ml). Phalloidin/methanol solution (5 μl per well) was diluted in BSA (1% in PBS, 2 ml) and added over night at 37 °C. After washing the gels twice with PBS, cells

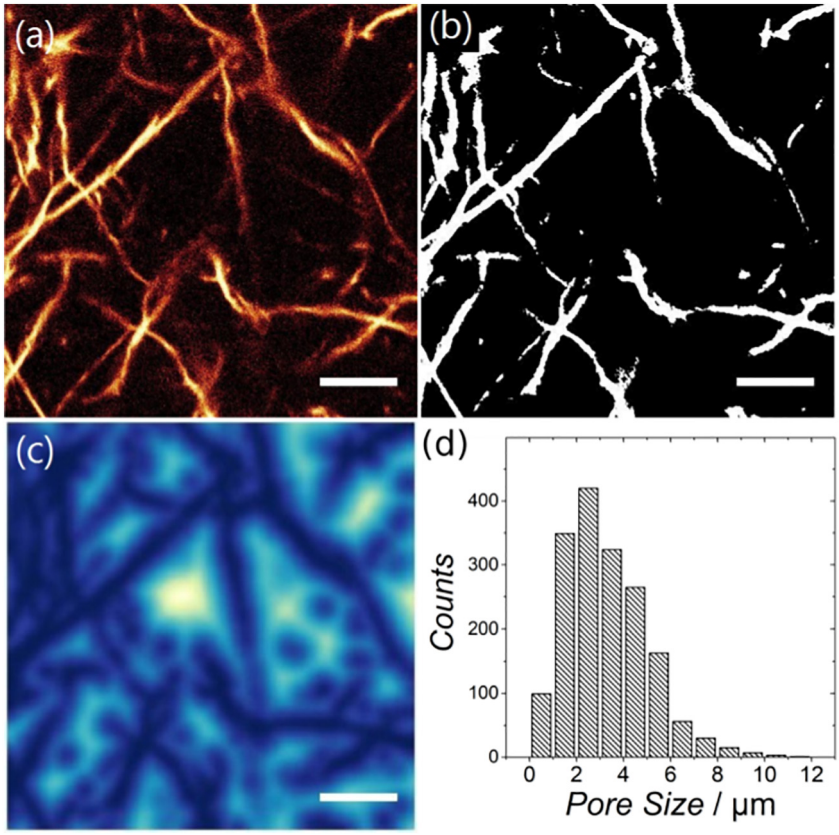

Fig. 1. Pore size determination: (a) 2D CLSM image of collagen network (2 mg/ml, 50 kGy). (b) Binary image. (c) 3D euclidean distance map of the CLSM image. The color indicates the distance to the nearest fiber: the brighter the color, the larger the distance. Local distance maxima represent the center of the pore. The euclidean distance at the local maximum defines the pore size of the pore. (d) Histogram of all calculated pore sizes of a collagen measurement. The characteristic pore size of the collagen network is defined as the average of the distribution. Scale bars represent 10 μm.

were imaged with a fluorescence microscope (Axio Scope A1; Carl Zeiss Microscopy GmbH, Germany) as well as by a spinning disk confocal microscope (CSU-X1A 5000; Yokogawa, Germany) combined with an inverted fluorescence microscope (Axio Observer.Z1; Carl Zeiss Microscopy GmbH).

To determine cellular viability, fluorescence flow cytometry measurements were performed. Cultivated cells were first harvested by dissolution of the collagen using Collagenase A (3 mg/ml, Cat. No. 10103578001; Sigma-Aldrich Chemie GmbH). Before Collagenase A was added, gels were washed twice with PBS. Then Collagenase A solution (1 ml) was added to collagen (2 ml) and incubated for 30 min. Afterwards, collagen was mechanically disintegrated by manual pipetting. After adding cell culture medium, the suspension was centrifuged as described above. The supernatant was removed and the obtained cells were stained with propidium-iodid (PI) and annexin *V* (V13242; Thermofischer) as suggested by the manufacturer. Cell viability was determined according to the manufacturer's recommendations. The number of viable, early apoptotic as well as late apoptotic and necrotic cells were determined using the flow cytometer LSRFortessa II (BD Biosciences, USA) and the data was analyzed using Flowing Software [50]. The experiment was repeated 3 times with each time 2 samples per irradiation dose and approx. 6000 analyzed cells per sample. Significance of viability of cells on irradiated gels compared to unirradiated (0 kGy) gels was tested by an independent two-sample *t*-test with 0.05 p-value.

3. Results and discussion

3.1. Chemical structure

Changes in the chemical structure of irradiated collagen were explored via Fourier Transform Infrared (FTIR) Spectroscopy. The obtained spectra (Fig. 2) show the characteristic amide peaks representing molecule-vibrations and -deformations. As shifts in the amide peak wavenumbers indicate changes in the secondary structure, e.g. transformations from helical to random coiled conformation, the wavenumbers of the amide peaks were determined as a function of irradiation dose (see Table 1).

In general, no large changes in the FTIR-spectra are observable; merely the amide A and II bands reveal a slight shift towards lower wavenumbers while the Amide *B*, *I* and III peaks remain constant. Thereby, the amide A band corresponds to N—H bond stretching and is located at 3305 cm^{-1} for the unirradiated collagen [51]. For higher doses (100 kGy), the peak shifts to 3283 cm^{-1} indicating a loss in helical content towards coiled structures [52]. Similar to the amide A, the amide II band shows a small shift from 1547 to 1535 cm^{-1}. In general, the amide II peak represents N—H bending and C—N stretching [52]. A shift to lower wavenumbers thus indicates a transformation from a helical to a random coiled structure as also seen in the amide A band. These results indicate that electron irradiation up to 100 kGy induces minor changes from helical to coiled structures. However, since the shifts are small and the amide B, I and III peaks do not change significantly, it indicates absence of degradation; viz. electron irradiated collagen still exhibits collagenous polymeric structures. Previous studies of electron beam treated collagen [43] observed similar results. Differences in the shift of single amide peaks, in particular of amide A, seem to be caused by the usage of different electron energies. The minor changes in chemical structure might indicate very careful modification of collagen upon treatment with energetic electrons which might be a result from a relatively low number of formed crosslinks per collagen molecule at the applied doses. An estimated number of crosslinks will be obtained via rheology derived crosslinking density calculations which are presented further on in the manuscript.

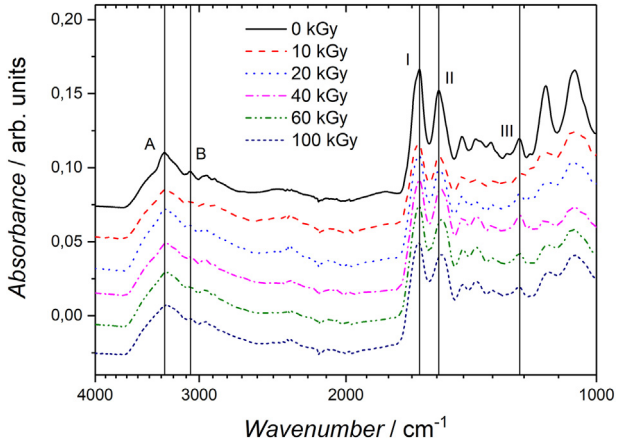

Fig. 2. FTIR spectra of electron irradiated collagen (gel concentration of 2 mg/ml). The marked peaks represent the characteristic amide peaks. Amid peak positions are listed in Table 1.

3.2. Network structure

Since the network structure has a direct impact on cellular response such as the ability of cells to migrate and invade the gels [53,54], the influence of electron irradiation on the pore size has to investigated. These changes in the structure of the collagen networks after electron beam treatment were studied by confocal laser scanning microscopy (CLSM) imaging and quantification of the characteristic network pore-size. Fig. 3 shows 2D images of 1, 2, and 3 mg/ml collagen irradiated with doses of 0, 50 and 100 kGy, respectively. It can be observed that the network pore size becomes smaller with increasing irradiation dose and collagen concentration. In addition, collagen pore sizes were quantitatively evaluated by 3D analysis of the CLSM images. The results are shown in Fig. 4.

The 3D image analysis revealed characteristic pore sizes of approx. 6, 4.5 and 4.25 μm for unirradiated collagens with concentrations of 1, 2 and 3 mg/ml, respectively. With an irradiation dose of 50 and 100 kGy, the pore size can be reduced to 75 and 50% of the initial size, respectively. Such a relative decrease in pore size was already reported for electron beam treated gelatin hydrogels [47] and is assigned to the introduction of inter-chain [55] and intra-chain crosslinks [43]. Densification is expected to be accompanied with changes in macroscopic geometry. In fact, global sample shrinkage was already observed by Wisotzki et al. [47] for gelatin and is presently documented for collagen within the Supporting Information Fig. S1. Its dependence on additional processing parameters, molecular origin and relation to observations during chemical crosslinking is currently explored and will be the focus of follow up studies.

With further examination, it becomes clear that the characteristic pore sizes are smaller than the average size of mammalian cells. However, cell migration is not excluded since cells might be very deformable. The most limiting factor of cell deformation is the cell nucleus which is the most rigid and undeformable part of the cell [56]. The average size of mammalian nuclei is 10–15 μm [57], which is still larger

Table 1
Amide peak position analysis of FTIR-measurements of irradiated collagen (2 mg/ml). The peak position was determined with an error of ±1 cm^{-1}.

Dose [kGy]	Amide Peak [cm^{-1}]				
	A	B	I	II	III
0	3305	3075	1632	1547	1238
10	3294	3074	1633	1545	1235
20	3294	3074	1631	1544	1237
40	3286	3074	1632	1537	1236
60	3284	3074	1632	1535	1238
100	3283	3074	1633	1535	1239

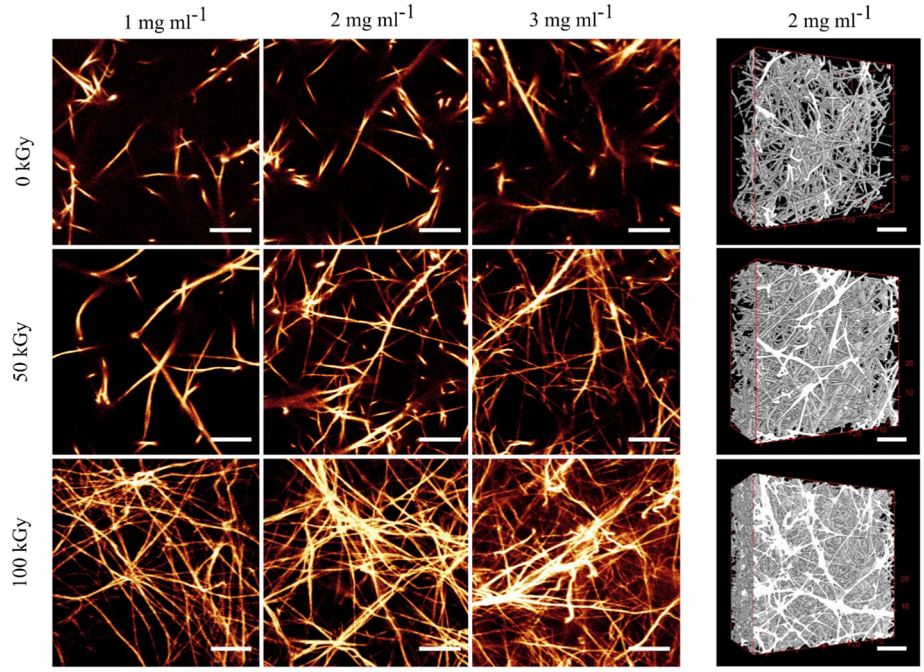

Fig. 3. Network structure of electron irradiated collagen with varying gel concentration as function of irradiation dose (0, 50 and 100 kGy). Left: Representative 2D images of 1, 2 and 3 mg/ml collagen gels. Right: Representative 3D images of 2 mg/ml collagen gels. Scale bars indicate 10 μm.

than the determined characteristic pore sizes. However, the collagen network is flexible enabling cells to migrate through the network. In addition, active matrix remodeling by cells further improves mobility of cells in theses matrices [58,59].

Since a densification as reported is expected to have an influence on the mechanical properties of the hydrogels, rheology measurements are discussed in the following.

3.3. Rheology

Next to the structure of the ECM network, also mechanical properties of the extracellular matrix might have an influence on cellular behavior [60]. Therefore, the effect of electron irradiation on the viscoelastic properties of collagen was investigated via oscillatory rheometer experiments. From here, the study was continued with doses up to 40 kGy since it was already observed that highly irradiated collagen gels become hard, brittle and show large shrinking. Therefore, they are clearly unsuitable as ECM model and are no longer in the focus of our study.

For a rheological study, storage and loss moduli were determined. The results are presented in Fig. 5. It can be observed that the electron assisted crosslinking technique leads to an increase in storage and loss moduli about one order of magnitude from approx. 50 to 500 Pa correlating well with biological tissue and tissue components [61].

This network stiffening and the decrease in viscosity are correlated with the irradiation induced crosslinking already described for hydrogels [62], collagen fibers [63] and gelatin hydrogels [47]. The introduced covalent bonds lead to an increased elastic modulus of the collagen fibrils and with this also of the entire network. This causes the release of water since the balance of swelling pressure and network stress is shifted and the transport of water into the hydrogel is hindered

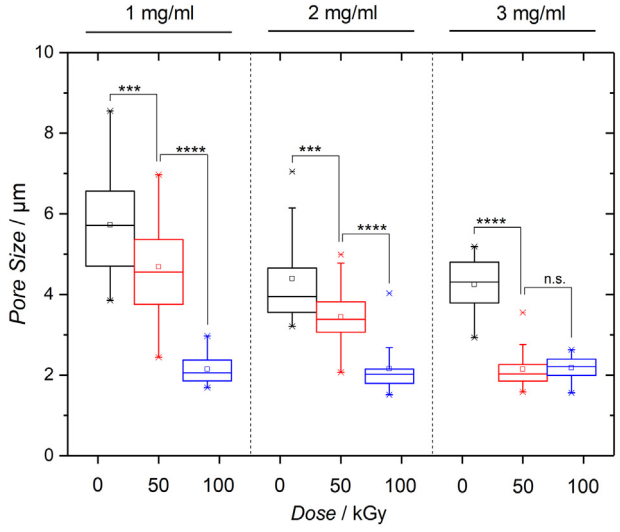

Fig. 4. Average pore size of collagen with varying gel concentration in dependence on the irradiation dose determined by 3D pore size analysis. Significance was tested by an independent two-sample *t*-test.

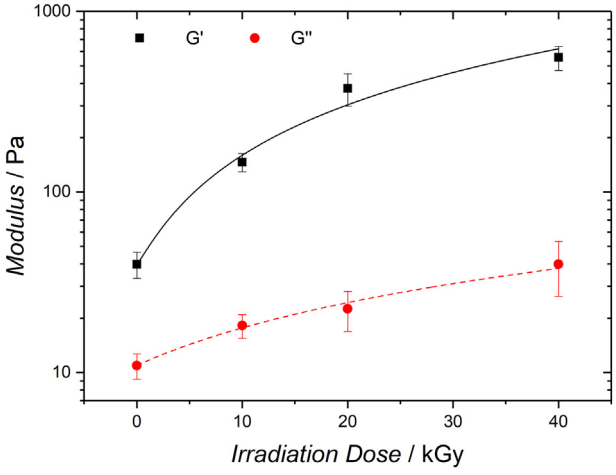

Fig. 5. Storage and loss moduli of electron irradiated collagen (2 mg/ml) in dependence on radiation dose, with power law fits. Error bars indicate standard deviation.

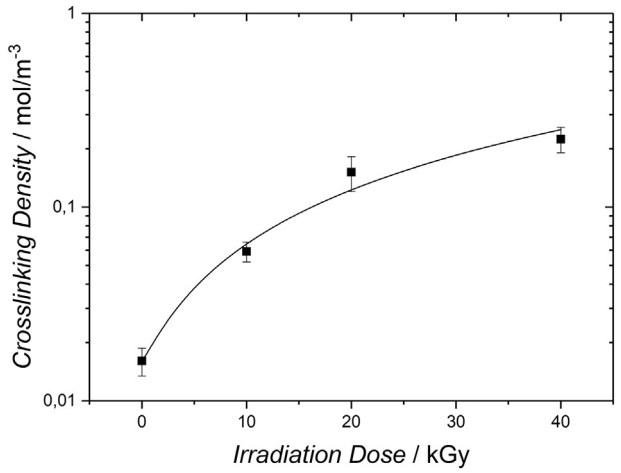

Fig. 6. Crosslinking density of electron irradiated collagen (2 mg/ml) determined via rubber elasticity theory (see Eq. (1)), with power law fit. Error bars indicate standard deviation.

with network stiffening. Together with the already mentioned densification, material stiffening is reasonable.

By using Eq. (1), the crosslinking density can be estimated as seen in Fig. 6. A linear correlation between irradiation dose and crosslinking density can be found for doses up to 60 kGy. It has to be taken into account that Eq. (1) applies in first approximation for collagen hydrogels since it is actually valid for an ideal rubber with purely elastic crosslinked polymer chains. For viscoelastic materials, contributions from trapped entanglements or network defects (loose chain ends, intramolecular loops, entangled chain loops) are not taken into account [64,65]. However, with this approximation which was already used for alcogels [66] or chitosan hydrogels [64] a qualitative estimation on changes in crosslinking density of electron crosslinked collagen can be made.

With the crosslinking density, the number of crosslinks per collagen molecules can be estimated. For example, for the 2 mg/ml collagen gels irradiated with 10 kGy, a crosslinking density of approx. 0.06 mol/m^3 corresponding to 2×10^{16} crosslinks per cm^3 collagen solution was determined. Taking into account that 1 cm^3 collagen solution (2 mg/ml) contains approx. 4×10^{15} collagen molecules (tropocollagen; molecular weight of 300 kDa), we can conclude that the ratio of collagen molecules to crosslinks is approx. 1:5, viz. 5 crosslinks per collagen molecule are introduced. This low number of introduced crosslinks might be the reason for the minor changes in the chemical structure of electron crosslinked collagen as observed by the earlier discussed FTIR measurements. However, these minor changes are still sufficient to precisely tailor material properties as demonstrated previously.

Besides, it should be noted that the rheology measurements were performed at 25 °C since the experimental setup was not able to measure at 37 °C. Earlier rheological studies on gelatin hydrogels [47] suggest slightly higher values for storage and loss modulus at 37 °C but an identical dose-modulus dependence. With this, the here presented measurements give a qualitatively good impression on the dose-modulus behavior of electron beam treated hydrogels also at human body temperature.

3.4. Cytocompatibility

To investigate cellular response on electron irradiated collagen gels, cells were cultured on these gels followed by cell imaging and viability tests using flow cytometry measurements. Fig. 7 shows fluorescence microscopy images of multiple and single NIH 3T3 fibroblasts cultured onto electron irradiated collagen gels with varying irradiation doses. We observed that the cultured cells invaded all collagen gels (not shown here). In addition, they exhibited characteristic cell morphology in 3D culture which is indicated by their elongated shape and

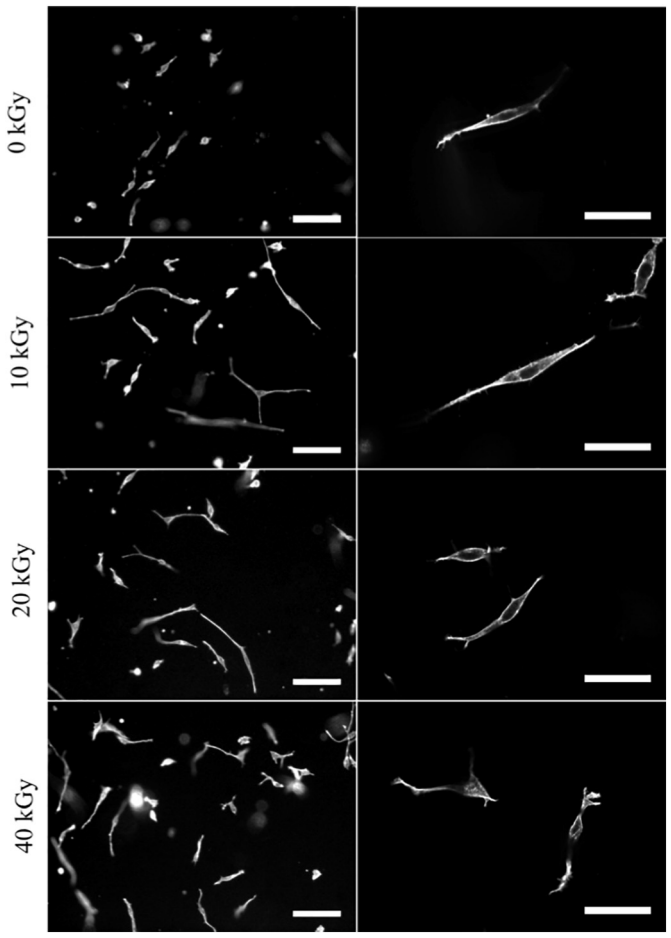

Fig. 7. Cellular response: NIH 3T3 fibroblasts after 48 h culture on electron irradiated collagen gels with varying irradiation doses visualized by actin staining. Left: Multiple cells imaged by fluorescent microscopy. Scale bars indicate 100 μm. Right: Single cells imaged using confocal fluorescent microscopy (laser scanning). Scale bars indicate 50 μm.

evolution of filopodia suggesting cellular viability [67]. It can be observed that the average cell shape shifts from a rather roundish shape on the soft unirradiated gels to a more elongated shape with a higher spread area for irradiated gels. This variation in cell shape may correlate with the matrix stiffness since cell morphology is affected by the mechanical properties of the substrate [68–72]. On all gels as well as the control sample, the cell density is similar giving a first indication that electron irradiated collagen gels are non-cytotoxic for NIH 3T3 fibroblasts. This qualitative investigation is examined in more detail by quantitative viability studies using flow cytometry measurements.

Viability tests were performed comparing NIH 3T3 fibroblasts which were cultured on the electron crosslinked collagen with respect to cells cultured on unirradiated collagen gels. Here, the percentage of viable, early apoptotic as well as late apoptotic and necrotic cells were determined via annexin V/propidium-iodid staining and flow cytometry measurement. The obtained results are presented in Fig. 8. These investigations show an excellent cellular viability of the fibroblasts, also on gels with higher irradiation doses of 40 kGy. Fibroblasts cultured on unirradiated as well as irradiated collagen how a viability of approx. 95% with 3% early apoptotic and 2% late apoptotic and necrotic cells with no significant differences. Compared to cells cultured on common cell culture dishes which showed a viability of approx. 97% (not shown here) the viability is not much decreased. This leads to the conclusion that electron irradiated collagen exhibits excellent cytocompatibility for NIH 3T3 cells and thereby represent promising materials for 3D culture substrates and candidates mimicking the ECM. Collagen generally has shown to be a good material for long-term culture of several cell

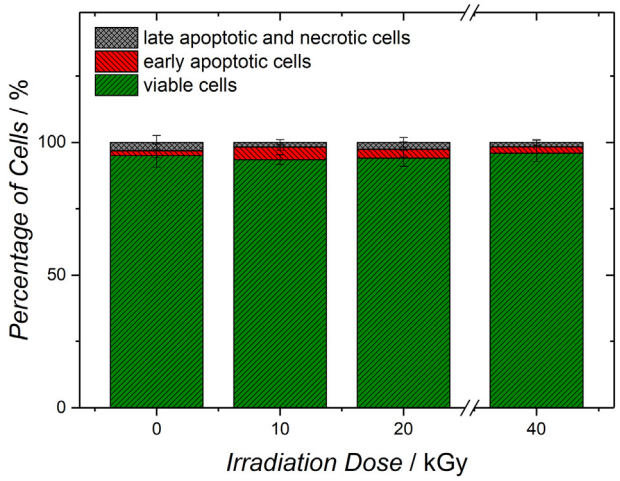

Fig. 8. Cellular viability: NIH 3T3 fibroblasts after 72 h culture on electron crosslinked collagen gels (2 mg/ml) as function of irradiation dose. The viability was determined by annexin V/Propidium-iodide staining and flow cytometry measurement. Error bars visualize standard deviation. Percentages of viable cells on irradiated gels were tested on significance compared to cells cultured on unirradiated collagen gels resulting in no significant differences.

lines for various applications without any toxic effect [73–77]. Since the electron irradiated hydrogels show no significant reduction in cellular viability over 3 days, it might be a promising material for long-term culture as well.

In addition, the ability of cells to invade the gels further indicates excellent biodegradability because fibroblast migration within the ECM and ECM models is usually accompanied by matrix remodeling via synthesis of matrix-proteases [78,79]. However, invasion behavior has to be investigated qualitatively and quantitatively in more detail in a follow up study.

If compared to other crosslinking techniques such as crosslinking via aldehydes (e.g. glutaraldehyde [80–83]), cellular viability is excellently maintained after electron beam treatment. The good cellular acceptance corresponds well to similar investigations on the cytotoxicity of NIH 3T3 fibroblasts on electron crosslinked gelatin [36] and suggests high cytocompatibility of electron irradiated collagen with potential as an excellent material for cell culture and other biomedical applications. This particularly includes mechanical tailoring of collagen-based organ scaffolds that have either been gained by decellularization from biological sources or modeled by 3D printing. However, no conclusion on in vivo biocompatibility can be made here at this point since natural proteins such as collagen often underlay restricted usage due to concerns regarding batch variations and induced immunogenic reactions. Although collagen is considered as a weak antigen, potential immune responses [84–86] must be kept in mind and in vivo applications have to be tested for the specific situation (material, patient, system etc.). This will be one of our future research directions.

4. Conclusions

In this study we demonstrate that electron beam assisted crosslinking is a promising reagent-free alternative to common crosslinking techniques. Electron treatment enables precise modification of collagen hydrogels towards controllable ECM model systems. FTIR measurements indicate that electron beam assisted crosslinking induces only minor changes, while the characteristic polymeric structure of collagen is maintained also for doses as high as 100 kGy. Pore size analysis indicates precise tunability of the network pore size. Rheological investigations show network stiffening over one order of magnitude indicating an increase in crosslinking density. Cell-experiments revealed an excellent cytocompatibility of electron irradiated collagen gels in terms of cellular viability.

With these investigations, we are able to show that high energy electron induced crosslinking presents a highly promising technique to tune collagen hydrogels in order to mimic ECM and other collagenous tissue by tailoring material characteristics such as structure and mechanics in a physiological relevant range while maintaining excellent cytocompatibility. These defined collagen systems represent 3D tissue models which are highly relevant in cell culture, as coatings or implants. They are also necessary to study cellular behavior in biomimetic tissue as in cancer research or to investigate drug delivery for pharmaceutical applications.

Our presented investigations are the basis for further studies on electron beam treated collagen matrices towards biomimetic scaffolds, which is possible globally (as in the present study) or locally (by utilizing a focused electron beam). Our next future steps have to examine long time cytocompatibility in vitro and in vivo as well as biocompatibility for clinical applications.

Supplementary data to this article can be found online at https://doi.org/10.1016/j.matdes.2019.107606.

Competing interests

We have no conflicts of interest to declare.

Funding

This work was supported by the DFG, Project “Biostrain” (MA 2432/5-1), as well as SMWK/SAB, Project “Biocoat” (100259192).

CRediT authorship contribution statement

Stefanie Riedel: Conceptualization, Methodology, Validation, Formal analysis, Investigation, Data curation, Writing - original draft, Writing - review & editing, Visualization, Supervision. **Philine Hietschold:** Conceptualization, Methodology, Validation, Formal analysis, Investigation, Data curation, Writing - original draft, Writing - review & editing, Visualization. **Catharina Krömmelbein:** Investigation, Validation, Formal analysis. **Tom Kunschmann:** Software, Data curation, Visualization. **Robert Konieczny:** Investigation, Writing - review & editing. **Wolfgang Knolle:** Investigation, Writing - review & editing. **Claudia T. Mierke:** Resources, Writing - review & editing, Supervision. **Mareike Zink:** Resources, Writing - review & editing, Supervision. **Stefan G. Mayr:** Conceptualization, Methodology, Supervision, Project administration, Funding acquisition, Resources, Writing - review & editing.

Acknowledgements

We thank Prof. Dr. J. A. Käs (Soft Matter Physics Division, University of Leipzig) for enabling us free access to his CLSM system as well as Dr. E. I. Wisotzki for valuable comments and suggestions, G. Mirschel for FTIR measurements and Dr. U. Müller (Core Unit Durchflusszytometrie CUDZ, College of Veterinary Medicine, University of Leipzig) for support with the flow cytometry measurements. This project was partially performed within the Leipzig Graduate School of Natural Sciences - Building with Molecules (BuildMoNa).

References

[1] N. Gjorevski, N. Sachs, A. Manfrin, S. Giger, M.E. Bragina, P. Ordóñez-Morán, H. Clevers, M.P. Lutolf, Nature 539 (2016) 560–564.
[2] A. Fatehullah, S.H. Tan, N. Barker, Nat. Cell Biol. 18 (2016) 246–254.
[3] A.J. Ryan, C.M. Brougham, C.D. Garciarena, S.W. Kerrigan, F.J. O'Brien, Drug Discov. Today 21 (2016) 1437–1445.
[4] S. Pradhan, J.M. Clary, D. Seliktar, E.A. Lipke, Biomaterials 115 (2017) 141–154.
[5] H.A.B. Multhaupt, B. Leitinger, D. Gullberg, J.R. Couchman, Adv. Drug Deliv. Rev. 97 (2016) 28–40.
[6] K. Panduranga Rao, J. Biomater. Sci. Polym. Ed. 7 (1996) 623–645.

[7] A.L. Rubin, K.H. Stenzel, T. Miyata, M.J. White, M. Dunn, J. Clin. Pharmacol. New Drugs 13 (1973) 309–312.
[8] R.A. Marklein, J.A. Burdick, Soft Matter 6 (2010) 136–143.
[9] A.J. Engler, M.A. Griffin, S. Sen, C.G. Bönnemann, H.L. Sweeney, D.E. Discher, J. Cell Biol. 166 (2004) 877–887.
[10] M.J. Dalby, N. Gadegaard, C.D.W. Wilkinson, J. Biomed. Mater. Res. A 84A (2008) 973–979.
[11] M.W. Tibbitt, K.S. Anseth, Biotechnol. Bioeng. 103 (2009) 655–663.
[12] G.D. Prestwich, K.E. Healy, Expert. Opin. Biol. Ther. 15 (2015) 3–7.
[13] R.J. Wade, J.A. Burdick, Mater. Today 15 (2012) 454–459.
[14] K.A. Kyburz, K.S. Anseth, Ann. Biomed. Eng. 43 (2015) 489–500.
[15] H.K. Kleinman, G.R. Martin, Semin. Cancer Biol. 15 (2005) 378–386.
[16] G. Benton, I. Arnaoutova, J. George, H.K. Kleinman, J. Koblinski, Adv. Drug Deliv. Rev. 79–80 (2014) 3–18.
[17] B.A. Roeder, K. Kokini, J.E. Sturgis, J.P. Robinson, S.L. Voytik-Harbin, J. Biomech. Eng. 124 (2002) 214.
[18] S. Hsu, A.M. Jamieson, J. Blackwell, Biorheology 31 (1994) 21–36.
[19] F. Gobeaux, G. Mosser, A. Anglo, P. Panine, P. Davidson, M.-M. Giraud-Guille, E. Belamie, J. Mol. Biol. 376 (2008) 1509–1522.
[20] M.E. Nimni, D. Cheung, B. Strates, M. Kodama, K. Sheikh, J. Biomed. Mater. Res. 21 (1987) 741–771.
[21] G.D. Pins, F.H. Silver, Mater. Sci. Eng. C 3 (1995) 101–107.
[22] B.P. Chan, T.Y. Hui, C.W. Yeung, J. Li, I. Mo, G.C.F. Chan, Biomaterials 28 (2007) 4652–4666.
[23] S.A. Sell, M.J. McClure, K. Garg, P.S. Wolfe, G.L. Bowlin, Adv. Drug Deliv. Rev. 61 (2009) 1007–1019.
[24] M.-T. Sheu, J.-C. Huang, G.-C. Yeh, H.-O. Ho, Biomaterials 22 (2001) 1713–1719.
[25] P. Lee, R. Lin, J. Moon, L.P. Lee, Biomed. Microdevices 8 (2006) 35–41.
[26] J.-P. Chen, G.-Y. Chang, J.-K. Chen, Colloids Surf. A Physicochem. Eng. Asp. 313–314 (2008) 183–188.
[27] S.M. Choi, H.A. Ryu, K.-M. Lee, H.J. Kim, I.K. Park, W.J. Cho, H.-C. Shin, W.J. Choi, J.W. Lee, Biomater. Res. 20 (2016) 1–7.
[28] A. Nyga, U. Cheema, M. Loizidou, J. Cell Commun. Signal. 5 (2011) 239–248.
[29] K. Weadock, R.M. Olson, F.H. Silver, Biomater. Med. Devices Artif. Organs 11 (1983) 293–318.
[30] J.M. Ruijgrok, J.R. de Wijn, M.E. Boon, Clin. Mater. 17 (1994) 23–27.
[31] L.H.H. Olde Damink, P.J. Dijkstra, M.J.A. Van Luyn, P.B. Van Wachem, P. Nieuwenhuis, J. Feijen, J. Mater. Sci. Mater. Med. 6 (1995) 460–472.
[32] Y. Di, R.J. Heath, Polym. Degrad. Stab. 94 (2009) 1684–1692.
[33] K. Reiser, R.J. McCormick, R.B. Rucker, FASEB J. 6 (1992) 2439–2449.
[34] E. Reichmanis, C.W. Frank, J.H. O'Donnell, D.J.T. Hill, in: E. Reichmanis, C.W. Frank, J.H. O'Donnell (Eds.), Irradiation of Polymeric Materials, 527, American Chemical Society, Washington, DC 1993, pp. 1–8.
[35] W.E. Hennink, C.F. van Nostrum, Adv. Drug Deliv. Rev. 64 (2012) 223–236.
[36] E.I. Wisotzki, R.P. Friedrich, A. Weidt, C. Alexiou, S.G. Mayr, M. Zink, Macromol. Biosci. 16 (2016) 914–924.
[37] G. Monaco, R. Cholas, L. Salvatore, M. Madaghiele, A. Sannino, Mater. Sci. Eng. C 71 (2017) 335–344.
[38] M. Hara, J. Oral Tissue Eng. 3 (2006) 118–124.
[39] F.F. Vieira, N.L. Del Mastro, Radiat. Phys. Chem. 63 (2002) 331–332.
[40] S. Riedel, B. Heyart, K.S. Apel, S.G. Mayr, Sci. Rep. 7 (2017) 17436.
[41] S. Riedel, S.G. Mayr, Phys. Rev. Appl. 9 (2018), 024011.
[42] S. Riedel, K. Bela, E.I. Wisotzki, C. Suckfüll, J. Zajadacz, S.G. Mayr, Mater. Des. 153 (2018) 80–85.
[43] B. Jiang, Z. Wu, H. Zhao, F. Tang, J. Lu, Q. Wei, X. Zhang, Biomaterials 27 (2006) 15–23.
[44] T. Kunschmann, S. Puder, T. Fischer, J. Perez, N. Wilharm, C.T. Mierke, Biochim. Biophys. Acta BBA - Mol. Cell Res. 1864 (2017) 580–593.
[45] T. Fischer, N. Wilharm, A. Hayn, C.T. Mierke, Converg. Sci. Phys. Oncol. 3 (2017), 044003.
[46] M.J. Paszek, N. Zahir, K.R. Johnson, J.N. Lakins, G.I. Rozenberg, A. Gefen, C.A. Reinhart-King, S.S. Margulies, M. Dembo, D. Boettiger, D.A. Hammer, V.M. Weaver, Cancer Cell 8 (2005) 241–254.
[47] E.I. Wisotzki, M. Hennes, C. Schuldt, F. Engert, W. Knolle, U. Decker, J.A. Käs, M. Zink, S.G. Mayr, J. Mater. Chem. B 2 (2014) 4297–4309.
[48] W. Mickel, S. Münster, L.M. Jawerth, D.A. Vader, D.A. Weitz, A.P. Sheppard, K. Mecke, B. Fabry, G.E. Schröder-Turk, Biophys. J. 95 (2008) 6072–6080.
[49] M. Ilavský, Responsive Gels: Volume Transitions I, 109, Springer, Berlin, Heidelberg, 1993 173–206.
[50] Perttu Terho, Flowing Software, http://flowingsoftware.btk.fi/ 2018.
[51] J.E. Mark (Ed.), Polymer Data Handbook, 2nd ed.Oxford University Press, Oxford; New York, 2009.
[52] A. Kamińska, A. Sionkowska, Polym. Degrad. Stab. 51 (1996) 19–26.
[53] J. Zeltinger, J.K. Sherwood, D.A. Graham, R. Müeller, L.G. Griffith, Tissue Eng. 7 (2001) 557–572.
[54] J. Park, D.-H. Kim, H.-N. Kim, C.J. Wang, M.K. Kwak, E. Hur, K.-Y. Suh, S.S. An, A. Levchenko, Nat. Mater. 15 (2016) 792–801.
[55] A.J. Bailey, Int. Rev. Connect. Tissue Res. 4 (1968) 233–281.
[56] F. Guilak, J.R. Tedrow, R. Burgkart, Biochem. Biophys. Res. Commun. 269 (2000) 781–786.
[57] S.G. Alam, D. Lovett, D.I. Kim, K.J. Roux, R.B. Dickinson, T.P. Lele, J. Cell Sci. 128 (2015) 1901–1911.
[58] L.M. Matrisian, Trends Genet. 6 (1990) 121–125.
[59] M. Larsen, V.V. Artym, J.A. Green, K.M. Yamada, Curr. Opin. Cell Biol. 18 (2006) 463–471.
[60] A.D. Doyle, K.M. Yamada, Exp. Cell Res. 343 (2016) 60–66.
[61] R. Akhtar, M.J. Sherratt, J.K. Cruickshank, B. Derby, Mater. Today 14 (2011) 96–105.
[62] J. Maitra, V.K. Shukla, Am. J. Polym. Sci. 4 (2014) 25–31.
[63] A.J. Bailey, D.N. Rhodes, C.W. Cater, Radiat. Res. 22 (1964) 606.
[64] H. Jiang, W. Su, P.T. Mather, T.J. Bunning, Polymer 40 (1999) 4593–4602.
[65] L.H. Sperling, Introduction to Physical Polymer Science, 4th ed. Wiley, Hoboken, N.J, 2006.
[66] A. Hajighasem, K. Kabiri, J. Polym. Res. 20 (2013) 218.
[67] E. Cukierman, Science 294 (2001) 1708–1712.
[68] T. Yeung, P.C. Georges, L.A. Flanagan, B. Marg, M. Ortiz, M. Funaki, N. Zahir, W. Ming, V. Weaver, P.A. Janmey, Cell Motil. Cytoskeleton 60 (2005) 24–34.
[69] D.E. Discher, Science 310 (2005) 1139–1143.
[70] I. Levental, P.C. Georges, P.A. Janmey, Soft Matter 3 (2007) 299–306.
[71] H.K. Heris, J. Daoud, S. Sheibani, H. Vali, M. Tabrizian, L. Mongeau, Adv. Healthc. Mater. 5 (2016) 255–265.
[72] F.M. Busra, Y. Lokanathan, M.M. Nadzir, A. Saim, R.B.H. Idrus, S.R. Chowdhury, Malays. J. Med. Sci. 24 (2017) 33–43.
[73] S. Nakagawa, P. Pawelek, F. Grinnell, J. Invest. Dermatol. 93 (1989) 792–798.
[74] M.G. Dunn, P.N. Avasarala, J.P. Zawadsky, J. Biomed. Mater. Res. 27 (1993) 1545–1552.
[75] T. Kimura, N. Yasui, S. Ohsawa, K. Ono, Clin. Orthop. (1984) 231–239.
[76] C. Dong, Y. Lv, Polymers 8 (2016) 42.
[77] A. Aravamudhan, D.M. Ramos, N.A. Jenkins, N.A. Dyment, M.M. Sanders, D.W. Rowe, S.G. Kumbar, RSC Adv. 6 (2016) 80851–80866.
[78] A.B. Pratt, F.E. Weber, H.G. Schmoekel, R. Müller, J.A. Hubbell, Biotechnol. Bioeng. 86 (2004) 27–36.
[79] M.P. Lutolf, J.L. Lauer-Fields, H.G. Schmoekel, A.T. Metters, F.E. Weber, G.B. Fields, J.A. Hubbell, Proc. Natl. Acad. Sci. 100 (2003) 5413–5418.
[80] J.E. Gough, C.A. Scotchford, S. Downes, J. Biomed. Mater. Res. 61 (2002) 121–130.
[81] L. Salvatore, M. Madaghiele, C. Parisi, F. Gatti, A. Sannino, J. Biomed. Mater. Res. A (2014) 4406–4414.
[82] A. Oryan, A. Kamali, A. Moshiri, H. Baharvand, H. Daemi, Int. J. Biol. Macromol. 107 (2018) 678–688.
[83] F. Garavand, M. Rouhi, S.H. Razavi, I. Cacciotti, R. Mohammadi, Int. J. Biol. Macromol. 104 (2017) 687–707.
[84] J. Zhu, R.E. Marchant, Expert Rev. Med. Devices 8 (2011) 607–626.
[85] A.K. Lynn, I.V. Yannas, W. Bonfield, J. Biomed. Mater. Res. 71B (2004) 343–354.
[86] R. Timpl, G. Wick, H. Furthmayr, C.M. Lapiere, K. Kuhn, Eur. J. Biochem. 32 (1973) 584–591.